

The rotational and physical properties of the Centaur (32532) 2001 PT₁₃

Tony L. Farnham^{a,*} and John K. Davies^b

^a Department of Astronomy, University of Texas, Austin, TX 78712, USA

^b Astronomy Technology Centre, Blackford Hill, Edinburgh, EH9 3HJ, UK

Received 2 July 2002; revised 30 April 2003

Abstract

We present observations of the Centaur (32532) 2001 PT₁₃ taken between September 2000 and December 2000. A multi-wavelength lightcurve was assembled from V-, R- and J-band photometry measurements. Analysis of the lightcurve indicates that there are two peaks of slightly different brightness, a rotation period of 0.34741 ± 0.00005 day, and a maximum photometric range of 0.18 mag. We obtained VRJHK colors ($V-R = 0.50 \pm 0.01$, $V-J = 1.69 \pm 0.02$, $V-H = 2.19 \pm 0.04$, and $V-K = 2.30 \pm 0.04$) that are consistent with the grey KBO/Centaur population. The V–R color shows no variation as a function of rotational phase; however, we cannot exclude the possibility that rotational variations are present in the R–J color. Assuming a 4% albedo, we estimate that 2001 PT₁₃ has an effective diameter of 90 km and a minimum axial ratio a/b of 1.18. We find no evidence of a coma and place an upper limit of 15 g s^{-1} on the dust production rate.

© 2003 Elsevier Inc. All rights reserved.

Keywords: Centaurs; Asteroids; Asteroids, rotation

1. Introduction

Centaurs are a relatively newly discovered class of minor bodies in the solar system, residing at heliocentric distances between Jupiter and Neptune. Due to gravitational interactions with the giant planets, their orbits are dynamically unstable, and this, combined with studies of the orbital evolution in the outer solar system, suggests that they represent a transition phase between transneptunian objects and short-period comets (Schulz, 2002, and references therein). Recent studies have confirmed that at least some Centaurs have ices on their surface (e.g., Cruikshank et al., 1998; Brown and Koresko, 1998; Foster et al., 1999; Luu et al., 2000; Kern et al., 2000; Bauer et al., 2002); however, 2060 Chiron and 2001 T₄ (Comet NEAT) are the only Centaurs known to exhibit cometary activity (e.g., Meech and Belton, 1989; Luu and Jewitt, 1990; Meech et al., 1997; Pravdo et al., 2001).

The Centaur (32532) 2001 PT₁₃ was discovered on 9 August 2001 by the Near Earth Asteroid Tracking program (NEAT); however, pre-discovery observations from 1995

and 1999 were subsequently found, which allowed a multiple-opposition orbit to be determined. We noted that this orbit, with an eccentricity $e = 0.2$ and a perihelion distance $q = 0.85$ AU, is similar to the orbits of Chiron and 2001 T₄, and so, if the objects are compositionally similar, 2001 PT₁₃ might be a good candidate for displaying cometary activity. Shortly after 2001 PT₁₃ was discovered, we started an observing program to search for evidence of activity and to determine other physical properties of the Centaur. From our earliest two nights of observations we were able to derive a rotation period of 0.35 day and a minimum axial ratio of 1.2 (Farnham, 2001a). The results presented here represent an analysis of our entire data set, spanning a time period of four months, and include a more precise measurement of the rotation period, as well as a more complete discussion of the rotational characteristics and VRJHK colors of 2001 PT₁₃.

2. Observations and data reduction

2.1. Optical data

Because our earliest observations showed lightcurve variations, we extended our program to allow us to assemble a lightcurve from which more accurate rotation characteristics could be determined. We obtained extensive observations

* Corresponding author.

E-mail address: farnham@astro.umd.edu (T.L. Farnham).

¹ Present address: Department of Astronomy, University of Maryland, College Park, MD 20742, USA.

Table 1
Summary of observations

UT date (2001)	Obs. site	r (AU)	Δ (AU)	α (deg)	λ (deg)	Filters	Seeing (arcsec)	Sky
03 Sep	UKIRT	8.856	7.903	2.3	332	J, H, K	< 1.0	Cirrus/clear
21 Sep	2.7-m	8.868	8.006	3.5	330	R	1.8	Cirrus
22 Sep	2.7-m	8.869	8.014	3.6	330	R, V	1.8	Cirrus
23 Sep	2.7-m	8.869	8.023	3.7	330	R, V	1.3	Photometric
24 Sep	2.7-m	8.870	8.032	3.7	329	R, V	2.0	Partly cloudy
10 Nov	2.7-m	8.903	8.661	6.3	329	R, V	1.9	Partly cloudy
11 Nov	2.7-m	8.903	8.678	6.3	329	R, V	1.5	Cirrus
12 Nov	2.7-m	8.904	8.694	6.3	329	R, V	1.3	Photometric
13 Nov	2.7-m	8.905	8.711	6.3	329	R, V	1.6	Cirrus
04 Dec	2.1-m	8.920	9.062	6.2	330	R, V	1.5	Cirrus
05 Dec	2.1-m	8.920	9.078	6.2	330	R, V	1.9	Cirrus
06 Dec	2.1-m	8.921	9.095	6.2	330	R, V	1.4	Partly cloudy

with V and R filters in September, November and December 2001 and with a J filter on 3 September 2001. A summary of the observing runs and geometric conditions is listed in Table 1. Each entry lists the date, observing site, heliocentric and geocentric distances, solar phase angle, ecliptic longitude, filters used, nominal seeing and a note about the quality of the observing conditions.

The data denoted “2.7-m” were obtained at the McDonald Observatory 2.7-m telescope with the Imaging Grism Instrument, a 5:1 focal reducer, and Harris V and Mould R filters. This configuration, combined with a TeK 1024 × 1024 CCD, results in a (vignetted) 7 arcmin field with 0.57 arcsec pixels. Data denoted “2.1-m” were obtained at the McDonald Observatory 2.1-m telescope, with the same instrumental setup and filters, producing a 7 arcmin field with 0.48 arcsec pixels. Observations typically consisted of alternating exposures with V and R filters, allowing a multi-wavelength lightcurve to be assembled and providing the information necessary for removing the lightcurve variations from the V–R color determination. The telescope was guided at the object’s rates and exposure times were limited so the stars would trail by less than half a pixel during an exposure. During most of these observations, the moon was either below the horizon or illuminated at less than 30%. The exception was on 4 December when the moon was 88% illuminated, though it rose halfway through our observations.

Processing of the V- and R-band images followed standard procedures and was done using the CCD reduction packages in the Image Reduction and Analysis Facility (IRAF). The bias was removed in two steps, first applying the overscan region to remove the bulk value, then subtracting off a master bias frame, created by averaging many bias images, to remove the residual for each individual pixel. Flat fielding was done using twilight sky flats, medianed together to remove any stars. Photometric measurements were obtained using the IRAF photometry packages. A 3-arcsec radius aperture was used for extracting magnitudes, with the sky background computed from an annulus with an inner radius of 10 arcsec and an outer radius of 20 arcsec. Pixels in this annulus whose values differed from the average by more than 2.5σ were removed from

the sample. Uncertainties in the instrumental magnitude include the uncertainty from variations in the sky background and the photon statistics in the signal above the background level.

Many of the observations were obtained under nonphotometric conditions. In order to incorporate all of the measurements into the lightcurve, we performed differential photometry using field stars as a photometric reference frame. The magnitude of 2001 PT₁₃ was measured in each frame, along with at least 10 stellar objects of varying magnitudes to act as comparison stars. Although 2001 PT₁₃ was moving too quickly to use the same stars throughout an entire observing run, it was moving slowly enough that at least half of the field of view overlapped from one night to the next. This allowed the same stars to be used for 2–3 nights, providing a link from one night to the next. The comparison star measurements were used to correct for the differing amounts of extinction for each frame (see Farnham, 2001b, for details).

On the nights of 24 September and 10 November the comparison stars apparently did not provide a complete correction to bring the lightcurve into alignment with other observations. Additional shifts of 0.08 mag on the 24 September and 0.06 mag on the 10 November data were needed to bring these nights’ lightcurves into agreement with the brightness on the other nights. We explored various potential explanations for these offsets, with no clear resolution. Stars of comparable brightness to 2001 PT₁₃ and stars distributed around the field of view are all well behaved, so it does not appear to be a degradation of the quality with different magnitudes or a problem with a particular region of the CCD. It does not appear to be due to 2001 PT₁₃ moving over a faint background star or galaxy because the object moves several aperture diameters during the observation period, and because coadding images from other nights shows no stars or galaxies along the path.

Both of these nights were of poor quality, so a combination of high extinction and poor seeing could be the cause of the offsets. To avoid any problems with the nonlinear extinction introduced by thick clouds, we discarded all measurements exhibiting more than 1 magnitude of extinction.

However, even if the analysis is done with only low extinction data (0.2–0.4 mag), the shift is still present. As for the image quality affecting the measurements, the 1.9–2.0 arcsec seeing on these nights, though poor, is not dramatically different from many of the other nights.

Because we couldn't find a specific cause for the offsets on 24 September and 10 November, we performed a re-analysis of the lightcurve with these two nights' observations left out, and found that the removal of the data has no effect on the final results. This is primarily because these nights represent only a small fraction of the total observations and their average uncertainties are larger than on other nights. When the lightcurve measurements are weighted by the uncertainties, these nights have relatively little influence on the result. Even though they have little impact, we include both nights' data, for completeness, in the analysis presented here, as well as in the figures and tables.

One night during each of the September and November runs was photometric, and on these nights, Landolt standard star fields (Landolt, 1992) were observed at a range of airmasses. These observations were used to compute the zero point of the instrumental magnitude and the extinction and color coefficients for that night. By this means, we were able to calibrate the comparison stars, which in turn were used to shift the 2001 PT₁₃ measurements to the standard photometric system. Although none of the December nights were photometric, we obtained calibration images of the field stars on a later observing run, allowing us to also calibrate the December magnitudes to the standard scale. The final observed magnitudes are listed in Table 2, where the observation times have been corrected for the light travel time and the midtime of the exposure. Note that the quoted magnitudes for 24 September and 10 November do not include the shifts that bring them into line with the other measurements.

The final step in assembling the lightcurve was to convert the measurements to absolute magnitudes H_V and H_R so that data from the different dates could be combined. To accomplish this, we removed the effects of changing distances by correcting the magnitudes to $r = 1$ AU and $\Delta = 1$ AU, and then removed the solar phase angle effects using the principles of the two-parameter (H, G) system of *Bowell et al. (1989)*. All of our measurements were obtained at solar phase angles of 3.5° – 3.7° , and 6.2° – 6.3° , which is too limited a data set to solve for G . Thus, we simply adopted the canonical value of $G = 0.15$ for correcting our observations to zero phase angle. As a check, we used the average lightcurve values from our September and November observing runs and found that they are consistent with our assumed value for G . (We have only sparse coverage of the lightcurve in our December data, so an average value cannot be reliably found for that time.) This gives us some confidence that our extrapolation to zero phase angle is not drastically in error.

2.2. Near IR data

The data denoted "UKIRT" were obtained at the 3.8-m United Kingdom Infrared Telescope on Mauna Kea, Hawaii, using the common user camera UFTI (UKIRT Fast Track Imager). The camera is equipped with a 1024×1024 HgCdTe array and has a plate scale of 0.09 arcsec per pixel, which gives a field of view of 92 arcsec. Observations were taken using standard filtering techniques to produce a median filtered flat-field as described in *Davies et al. (1998a)*. Each final UFTI image of 2001 PT₁₃ comprises a mosaic of 9 frames of 60 s each, for a total of 540 s per final image. Tip-tilt guiding on a suitable reference star was used during the observations to maximize image quality.

Thin cirrus was present during the first half of the night, so differential photometry was again used to incorporate all of the data. Initially, two field stars were used as the photometric reference, but it was later determined that one of them had a faint companion, so it was rejected as a comparison star. At the time of the observation, 2001 PT₁₃ was moving at 0.19 arcsec/min, trailing by approximately 1.8 arcsec during the 9-min mosaic. Relative photometry techniques using small apertures require that both target and comparison stars have identical point spread functions, so we processed each set of images twice, once in the sidereal frame and once in the moving frame of the Centaur. Reduction and mosaicking were done automatically using the UKIRT telescope's ORAC data reduction package, which registers stars automatically during mosaicking and can then apply appropriate tracking rates as required (*Bridger et al., 2000; Currie, 2001*). Photometry of 2001 PT₁₃ was done using the mosaic reconstructed in the moving frames, while the reference stars were measured in the fixed frame. This removes much of the effect of trailing, but the motion of the Centaur during each 60-s exposure cannot be completely negated by this process, so it will always be trailed over two of the UFTI 0.09 arcsec pixels. However, this is a factor of 3–4 less than the typical seeing during the night and only 7% of the 30 pixel diameter aperture used for the relative photometry.

As the moon was full during these observations, we were able to monitor the observing conditions. The sky cleared after midnight and the standard stars FS29 and FS11 from the list of *Hawarden et al. (2001)* were observed. Absolute calibration of the reference star was done using an aperture of 5 arcsec diameter (56 pixels) on a number of the sidereal mosaics. The reference star was then used to calibrate the 2001 PT₁₃ measurements. The final observed IR magnitudes are listed in Table 2, and again, the observation times have been corrected to the Centaur's reference frame. To incorporate these magnitudes into the lightcurve and to compute the VRJHK colors, we applied corrections for the solar phase angle (again assuming $G = 0.15$) and the changing heliocentric and geocentric distances as discussed in the optical section above.

Table 2
Photometry of 2001 PT₁₃

Julian day	Filter	mag	σ	Julian day	Filter	mag	σ	Julian day	Filter	mag	σ
3 September 2001				22 September 2001 (<i>continued</i>)				23 September 2001 (<i>continued</i>)			
2452155.6845	J	17.145	0.020	2452174.7364	R	18.489	0.011	2452175.7776	R	18.502	0.011
2452155.6920	J	17.121	0.020	2452174.7457	R	18.482	0.009	2452175.7817	V	18.978	0.011
2452155.7021	J	17.192	0.020	2452174.7509	R	18.517	0.010	2452175.7859	R	18.523	0.011
2452155.7097	J	17.093	0.020	2452174.7555	R	18.479	0.008	2452175.8109	R	18.532	0.009
2452155.7172	J	17.045	0.020	2452174.7601	R	18.509	0.019	2452175.8150	V	19.032	0.010
2452155.7258	J	16.985	0.020	2452174.7646	R	18.528	0.023	2452175.8365	R	18.472	0.009
2452155.7333	J	17.012	0.020	2452174.7690	R	18.501	0.016	2452175.8406	V	18.975	0.012
2452155.7409	J	17.037	0.020	2452174.7733	R	18.505	0.010	2452175.8448	R	18.437	0.010
2452155.7488	J	17.002	0.020	2452174.7779	R	18.491	0.011	2452175.8490	V	18.923	0.012
2452155.7564	J	17.029	0.020	2452174.7838	R	18.472	0.007	2452175.8532	R	18.411	0.010
2452155.7640	J	17.044	0.020	2452174.7880	R	18.470	0.008				
2452155.7715	J	16.983	0.020	2452174.7921	R	18.444	0.008	24 September 2001			
2452155.7792	J	17.043	0.020	2452174.7967	R	18.462	0.012	2452176.6430	R	18.474	0.011
2452155.7868	J	17.131	0.020	2452174.8011	R	18.433	0.011	2452176.6485	V	18.989	0.011
2452155.8130	J	17.213	0.020	2452174.8053	R	18.408	0.010	2452176.6527	R	18.465	0.013
2452155.8207	H	16.651	0.050	2452174.8094	R	18.398	0.010	2452176.6827	R	18.453	0.010
2452155.8283	J	17.161	0.020	2452174.8138	R	18.376	0.008	2452176.6869	V	18.977	0.011
2452155.8360	K	16.533	0.050	2452174.8184	R	18.346	0.008	2452176.6911	R	18.467	0.009
2452155.8436	J	17.137	0.020	2452174.8232	R	18.332	0.009	2452176.6952	V	18.974	0.010
2452155.8616	J	17.055	0.020	2452174.8273	R	18.363	0.010	2452176.6995	R	18.452	0.009
2452155.8693	H	16.588	0.050	2452174.8321	R	18.329	0.010	2452176.7244	R	18.396	0.010
2452155.9101	J	17.008	0.020	2452174.8362	R	18.328	0.011	2452176.7286	V	18.892	0.010
2452155.9178	K	16.375	0.050	2452174.8403	R	18.295	0.010	2452176.7329	R	18.357	0.015
2452155.9254	J	16.931	0.020	2452174.8444	R	18.321	0.009	2452176.7371	V	18.826	0.011
2452155.9355	J	17.029	0.020	2452174.8487	R	18.318	0.013	2452176.7416	R	18.371	0.010
2452155.9526	J	17.046	0.020	2452174.8531	R	18.293	0.011	2452176.7457	V	18.841	0.010
2452155.9601	J	17.120	0.020	2452174.8573	R	18.289	0.013	2452176.7499	R	18.366	0.012
2452155.9677	J	17.143	0.020	2452174.8615	R	18.330	0.012	2452176.7540	V	18.835	0.011
2452155.9953	J	17.148	0.020					2452176.7581	R	18.367	0.010
				23 September 2001				2452176.7622	V	18.845	0.010
21 September 2001				2452175.5423	R	18.318	0.013	2452176.7666	R	18.362	0.009
2452173.7256	R	18.504	0.010	2452175.5468	V	18.807	0.013	2452176.8079	R	18.488	0.013
2452173.7291	R	18.504	0.010	2452175.5511	R	18.312	0.012	2452176.8122	V	18.968	0.012
2452173.7320	R	18.499	0.011	2452175.5554	V	18.811	0.015	2452176.8164	R	18.484	0.013
2452173.7367	R	18.460	0.012	2452175.5599	R	18.314	0.014	2452176.8206	V	19.030	0.021
2452173.7421	R	18.453	0.007	2452175.5640	V	18.830	0.016	2452176.8248	R	18.572	0.039
				2452175.5683	R	18.325	0.012	2452176.8367	R	18.476	0.014
22 September 2001				2452175.6028	R	18.510	0.014	2452176.8408	R	18.472	0.019
2452174.5694	R	18.495	0.008	2452175.6075	V	18.984	0.012	2452176.8451	V	18.974	0.020
2452174.5734	R	18.489	0.009	2452175.6119	R	18.484	0.012	2452176.8492	R	18.493	0.032
2452174.5796	R	18.525	0.008	2452175.6166	V	18.991	0.011	2452176.8534	V	19.034	0.066
2452174.5879	R	18.535	0.010	2452175.6212	R	18.485	0.012	2452176.8575	R	18.455	0.029
2452174.6280	R	18.403	0.006	2452175.6255	V	19.004	0.013				
2452174.6373	R	18.359	0.013	2452175.6298	R	18.480	0.011	10 November 2001			
2452174.6496	R	18.348	0.008	2452175.6340	V	18.997	0.020	2452223.5235	R	18.675	0.008
2452174.6550	R	18.348	0.007	2452175.6386	R	18.473	0.018	2452223.5315	V	19.179	0.009
2452174.6599	R	18.328	0.008	2452175.6429	V	19.053	0.023	2452223.5455	R	18.780	0.007
2452174.6652	R	18.353	0.010	2452175.6474	R	18.519	0.012	2452223.5524	V	19.313	0.007
2452174.6700	R	18.342	0.012	2452175.6572	R	18.452	0.008	2452223.5604	R	18.804	0.008
2452174.6743	R	18.324	0.014	2452175.6614	V	18.905	0.013	2452223.5950	R	18.676	0.029
2452174.6875	R	18.372	0.017	2452175.6655	R	18.438	0.011	2452223.6204	R	18.716	0.015
2452174.6921	R	18.395	0.013	2452175.6697	V	18.901	0.010	2452223.6284	R	18.661	0.023
2452174.6995	R	18.412	0.011	2452175.6741	R	18.388	0.009	2452223.6364	V	19.158	0.012
2452174.7044	R	18.383	0.010	2452175.7250	R	18.366	0.007	2452223.6444	R	18.673	0.010
2452174.7088	R	18.360	0.015	2452175.7291	V	18.889	0.011	2452223.6888	R	18.707	0.050
2452174.7131	R	18.428	0.014	2452175.7333	R	18.387	0.008				
2452174.7181	R	18.461	0.009	2452175.7374	V	18.897	0.010	11 November 2001			
2452174.7229	R	18.470	0.007	2452175.7416	R	18.402	0.008	2452224.5114	R	18.668	0.007
2452174.7273	R	18.481	0.007	2452175.7691	R	18.461	0.012	2452224.5194	V	19.157	0.017
2452174.7318	R	18.502	0.010	2452175.7733	V	18.989	0.011	2452224.5274	R	18.657	0.007

(continued on next page)

Table 2 (continued)

Julian day	Filter	mag	σ	Julian day	Filter	mag	σ	Julian day	Filter	mag	σ
11 November 2001 (continued)				12 November 2001 (continued)				13 November 2001 (continued)			
2452224.5344	V	19.151	0.009	2452225.5875	R	18.679	0.008	2452226.5954	V	19.183	0.010
2452224.5434	R	18.695	0.053	2452225.5915	V	19.191	0.008	2452226.5994	R	18.660	0.008
2452224.5524	R	18.680	0.006	2452225.5965	R	18.698	0.007	2452226.6044	V	19.099	0.013
2452224.5604	V	19.203	0.007	2452225.6005	R	18.702	0.007	2452226.6084	R	18.664	0.013
2452224.5684	R	18.722	0.007	2452225.6055	R	18.697	0.007	2452226.6124	V	19.135	0.018
2452224.5764	V	19.255	0.007	2452225.6095	V	19.224	0.009	2452226.6164	R	18.667	0.010
2452224.5834	R	18.780	0.006	2452225.6135	R	18.705	0.007	2452226.6214	V	19.152	0.011
2452224.6276	R	18.775	0.014	2452225.6505	R	18.896	0.012	2452226.6254	R	18.670	0.012
2452224.6316	V	19.285	0.030	2452225.6545	V	19.370	0.015	2452226.6294	V	19.208	0.018
2452224.6376	R	18.771	0.008	2452225.6645	R	18.827	0.009	2452226.6334	R	18.647	0.019
2452224.6416	V	19.271	0.010	2452225.6685	V	19.320	0.012	2452226.6374	V	19.172	0.012
2452224.6456	R	18.750	0.008	2452225.6725	R	18.802	0.010	2452226.6424	R	18.691	0.011
2452224.6496	V	19.287	0.011	2452225.6775	V	19.305	0.014	2452226.6474	V	19.217	0.016
2452224.6546	R	18.716	0.008	2452225.6815	R	18.775	0.009	2452226.6514	R	18.690	0.011
2452224.6586	V	19.211	0.011	2452225.6855	V	19.284	0.013	2452226.6554	V	19.245	0.016
2452224.6626	R	18.712	0.008	2452225.6905	R	18.724	0.009	2452226.6594	R	18.757	0.020
2452224.6666	V	19.223	0.012	2452225.6945	V	19.256	0.014	2452226.6652	R	18.786	0.014
2452224.6716	R	18.715	0.009	2452225.6985	R	18.692	0.010	2452226.6714	R	18.774	0.014
2452224.6756	V	19.198	0.013	2452225.7025	R	18.672	0.011	2452226.6754	R	18.779	0.014
2452224.6806	R	18.676	0.010	2452225.7075	V	19.113	0.015	2452226.6794	R	18.776	0.011
2452224.6846	V	19.196	0.012	2452225.7115	R	18.622	0.011	2452226.6844	R	18.791	0.013
2452224.6896	R	18.652	0.009					2452226.6884	R	18.869	0.051
2452224.6936	V	19.143	0.013	13 November 2001				2452226.6924	R	18.804	0.017
2452224.6976	R	18.646	0.010	2452226.4904	R	18.756	0.012	2452226.6964	R	18.796	0.018
2452224.7026	V	19.181	0.016	2452226.4944	V	19.271	0.014	2452226.7004	R	18.804	0.017
2452224.7066	R	18.690	0.011	2452226.4984	R	18.798	0.009	2452226.7044	R	18.802	0.019
2452224.7116	V	19.202	0.020	2452226.5024	V	19.283	0.010	2452226.7104	R	18.795	0.018
2452224.7166	R	18.659	0.016	2452226.5074	R	18.805	0.008	4 December 2001			
				2452226.5114	V	19.293	0.011	2452247.5376	R	18.896	0.012
12 November 2001				2452226.5154	R	18.805	0.010	2452247.5460	V	19.411	0.013
2452225.4993	R	18.807	0.006	2452226.5194	V	19.333	0.012	2452247.5526	R	18.855	0.015
2452225.5073	V	19.315	0.008	2452226.5234	R	18.821	0.009	2452247.5572	R	18.889	0.017
2452225.5175	R	18.781	0.009	2452226.5274	V	19.331	0.010	2452247.5614	V	19.427	0.019
2452225.5225	V	19.275	0.009	2452226.5324	R	18.825	0.008	2452247.5656	R	18.930	0.020
2452225.5265	R	18.741	0.008	2452226.5364	V	19.333	0.010	5 December 2001			
2452225.5315	V	19.225	0.009	2452226.5404	R	18.818	0.008	2452248.5417	R	18.851	0.014
2452225.5365	R	18.713	0.007	2452226.5444	V	19.331	0.010	2452248.5459	V	19.357	0.012
2452225.5405	V	19.202	0.009	2452226.5484	R	18.820	0.008	2452248.5504	R	18.845	0.014
2452225.5445	R	18.705	0.007	2452226.5534	V	19.298	0.012	2452248.5546	V	19.351	0.014
2452225.5485	V	19.189	0.009	2452226.5574	R	18.802	0.009	2452248.5589	R	18.891	0.014
2452225.5535	R	18.658	0.007	2452226.5614	V	19.300	0.011	6 December 2001			
2452225.5585	V	19.181	0.009	2452226.5654	R	18.780	0.008	2452249.5717	V	19.280	0.021
2452225.5625	R	18.663	0.007	2452226.5694	V	19.245	0.010	2452249.5759	R	18.693	0.026
2452225.5665	V	19.176	0.008	2452226.5744	R	18.721	0.007				
2452225.5705	R	18.664	0.007	2452226.5784	V	19.214	0.009				
2452225.5745	V	19.171	0.008	2452226.5824	R	18.692	0.008				
2452225.5785	R	18.651	0.007	2452226.5874	V	19.206	0.009				
2452225.5835	V	19.164	0.008	2452226.5914	R	18.680	0.010				

3. Analysis

3.1. Rotation period

In the case of outer solar system objects, long orbital periods mean there is usually little change in the viewing geometry over a period of many months. For 2001 PT₁₃ the ecliptic longitude, λ , changed by only about 3° and the phase angle changed by only about 4° during our observations (see Table 1), both primarily due to the reflex motion of the Earth. The nearly constant viewing geometry means that we can

combine all of our data into a single phased lightcurve, without needing to know the orientation of the spin axis. This allows us to utilize the full time baseline spanned by our data to find a more precise measurement of the rotation period.

We analyzed the variations in the lightcurve of 2001 PT₁₃ using the phase dispersion minimization (PDM) technique (Stellingwerf, 1978). With this technique, the data are systematically phased to different periods, and the amount of scatter is computed for each case. The most likely period is the one that produces the smallest amount of scatter in the phased lightcurve. We implemented the same basic ap-

proach as described by Stellingwerf, but with modifications that allow the data to be weighted by their uncertainties.

In order to include all three lightcurves (R, V and J) into our analysis of the rotation period, it was necessary to take the color differences into account. First, we started with our R-band data and solved for the best period. The V-band data were then phased to the same period and shifted vertically until they matched the R lightcurve. With the combined R and V lightcurves, we again solved for the best period. This process was iterated until the result converged; however, we note that the period determination was not very sensitive to the exact vertical alignment of the R and V lightcurves. The J-band data were then incorporated in the same manner, giving us a time baseline of more than three full months for the period determination. After the best period had been determined, we estimated the uncertainty by increasing and decreasing the period until the phasing of the data was noticeably poorer than at the optimum period. This method overshoots the true uncertainty in the period but allows us to at least provide a quantitative estimate of the errors.

After systematically exploring periods from 0.01 to 2 days, we found the rotation period that produces the least amount of scatter in the phased lightcurve was 0.34741 ± 0.00005 day. Figure 1 shows this double-peaked lightcurve, corrected to the absolute magnitude (H_R) system and phased to the optimum rotation period. Zero phase was assigned to JD 2452173.72214 to correspond to a minimum between the peaks. As can be seen in the lightcurve, the two peaks have slightly different brightnesses. By taking the weighted average of the points within ± 0.025 phase of each peak, we find that the first peak is 0.03 mag brighter than the second. It's possible that the two minima also have slightly different brightnesses, but, given the noise levels, this is not conclusive. The maximum peak-to-peak extreme of the lightcurve (as measured between 0 and 0.25 phase) is 0.18 mag.

3.2. VRJK colors

We computed the V–R colors using two different methods. The first technique comes directly from the process of assembling the lightcurve, described above. In this case, we shifted the V magnitudes to match the R values, and the amount of shift gives the V–R color averaged over the entire lightcurve. In the second method, we use a set of three measurements—two Rs bracketing a V—to compute two measures of the color. Averaging these two values, to first order, removes the effects of the lightcurve variation, giving a single V–R color for that set of observations. This process is repeated for all sets in which two R-measurements bracket a V, and all of the individual color values are ultimately combined to obtain a global average of V–R. In principle, both techniques should converge on the same color, but with limited data sets, application of both techniques can reveal potential skewing effects in one or both measurements. For example, if there are color variations in the lightcurve as a

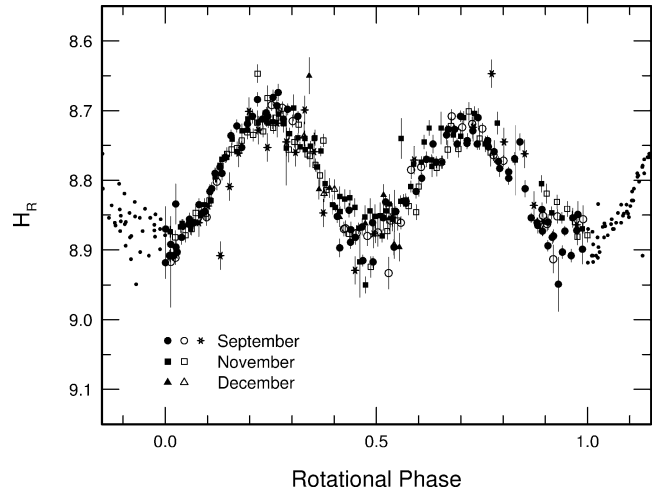


Fig. 1. 2001 PT₁₃ data from 2001 phased to a period of 0.34741 day. The symbol types denote different observing runs, with R-band data marked as solid points and V- and J-band data, shifted to match the R-lightcurve (0.50 and 1.19 mag, respectively), marked as open points and stars. Zero phase is defined at JD 2452173.72214.

function of rotational phase, then the vertical shift needed to align the lightcurves can be affected by the sampling of the data and/or the fact that lightcurve minima tend to be noisier than maxima. Similarly, data points that don't follow the R–V–R format are not included in the second method of determining the color, which means the two techniques utilize slightly different data sets, and can produce different results in the average colors. By computing the colors with both techniques, we can compare the results and initiate a more detailed investigation if the results don't agree. In the case of our optical measurements of 2001 PT₁₃, we found that the colors derived from the two techniques are consistent, with both producing an average value $V-R = 0.50 \pm 0.01$.

We do not have simultaneous measurements with R and J filters. Therefore, in order to compute the near-IR color, it was necessary to assume that the magnitudes did not change dramatically between 3 September and 23 September, when the near-IR and R measurements, respectively, were obtained. We then used the first method described above, phasing the J measurements to our best rotation period and then shifting vertically to align the J lightcurve with the R lightcurve. The magnitude of the shift represents an average color $R-J = 1.19 \pm 0.02$. We also have two observations each through H and K filters. Using J-band measurements bracketing these observations, we computed the average color indices $J-H = 0.50 \pm 0.04$ and $J-K = 0.61 \pm 0.04$. These colors then lead to an $H-K = 0.11 \pm 0.05$. We also note that the difference in magnitudes between the individual pairs of measurements through the H and K filters is consistent with the expected magnitude change from the lightcurve for the corresponding phases. Thus, variations in the near-IR data agree, at least to first order, with the lightcurve we observed in the optical.

To investigate possible color variations as a function of rotational phase, we utilized the temporal information in our

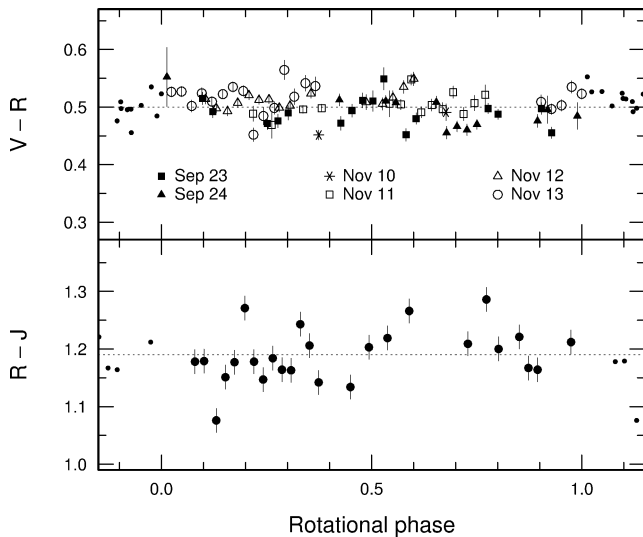


Fig. 2. V–R and R–J colors for 2001 PT₁₃ as a function of rotational phase (see caption for Fig. 1). In the top panel, each point represents the average of a pair of measurements in an R, V, R sequence, which removes the effects introduced by lightcurve variations. The different symbols represent measurements from different nights, as indicated. In the bottom panel, each point represents an R–J measurement, where the R magnitude has been obtained from the lightcurve at the phase corresponding to the measured J-band value. In both plots, the dotted line denotes the average color.

data. For V–R, we used the colors computed for each R–V–R data set, and phased them to our best rotation period. The results are shown in the top panel of Fig. 2. A visual inspection of this result reveals no obvious variation with rotational phase.

For R–J, we computed the phase at which each of the J observations was obtained and used the average R magnitude at that phase to compute the color. The results are plotted in the bottom panel of Fig. 2. In this case, we note that from phase 0 to 0.5, most of the measurements are concentrated below the average, while from phase 0.5 to 1.0, the colors tend to lie above the average. As an exercise, we fit a sine curve to the data and found that the best fit occurred when the curve had an amplitude of 0.03 mag. This suggests that the R–J color may vary with rotation, though with the amount of scatter and the lack of simultaneous R and J observations, this is by no means conclusive.

Pursuing this issue further, we performed a test to determine whether a flat color distribution could be excluded, based on the distribution of the data. Our measurements consist of 25 data points, well distributed in rotational phase and exhibiting a scatter in the color with a standard deviation $\sigma = 0.047$ mag. If we divide the data into the two phase bins described above, we find that the average color of one bin is approximately 1σ greater than the other. Using this information as a guide, we utilized a Monte-Carlo model to determine the likelihood that the data groupings were produced by chance. In our model, we produced a synthetic data set of 25 points randomly distributed in phase, with colors following a Gaussian distribution ($\sigma = 0.047$ mag). We divided the synthetic data into two bins, each of which covers half

a rotation, and computed the average color in each bin. (To avoid prespecifying where the two phase bins were located, we allowed the bins to slide in phase until the difference in the two average colors reached a maximum.) We performed 10,000 runs with this model, and found that in 5% of the cases, one bin had an average color that was $\geq 1\sigma$ higher than the other. This frequency is high enough that we cannot rule out the possibility that the color is flat with rotation.

Finally, we attempted to determine the magnitude of potential color variations that could be present and still be consistent with our observations. For this investigation, we assumed the variations take the form of a sine wave with three free parameters (amplitude, phase offset and offset from the average color). As stated earlier, the minimum χ^2 fit to the R–J colors was obtained for a curve with amplitude 0.03 mag. In comparison, a flat color relation had a χ^2 that was 20% higher for the same data set. Because the flat color relation is consistent with our observations, we adopted this range of 20% above the minimum as the limit for which χ^2 represents an acceptable fit to the data. We then performed a full grid search of parameter space to find the largest amplitude that still produced an acceptable χ^2 value. For the R–J colors, we find that a sine curve variation with an amplitude as high as 0.06 mag will fit the data as well as the flat relation. Using the same analysis on the visible colors, we find a best fit for a curve with no amplitude, suggesting that the V–R color relation is, indeed, flat. If we again utilize the 20% above minimum χ^2 level as our range of acceptable fits, then an amplitude of 0.02 mag is the maximum that remains consistent with our measurements.

3.3. Search for cometary activity

Because 2001 PT₁₃ has an orbit similar to those of Chiron and 2001 T₄, it has the potential for exhibiting cometary activity. To investigate this possibility, we thoroughly searched our images for evidence of coma. None was visible in individual images at either the V- or R-band wavelengths, but a low surface brightness coma could easily be lost in the sky noise of the short-exposure images. To improve the signal and allow us to search for faint coma, we co-added all of the data from 23 September 2001 and from 12 November 2001. These nights were selected because they were photometric, had the best seeing of their respective observing runs, and had a large number of images. Before coadding the images, it was necessary to shift each frame to position the object at a common location. For each image, the required shift was computed in two stages. First, measurements of 10–20 stars allowed us to accurately compute the shift needed to align the star field. Then the nonsidereal motions of 2001 PT₁₃, computed from the ephemeris rates and the known pixel scale, were added to the star shifts. After the images were shifted, they were added together by filter type. Because of the object's motion, the stars in the composite images were trailed. Therefore, we shifted the original images a second time to align the stars into a separate composite from which

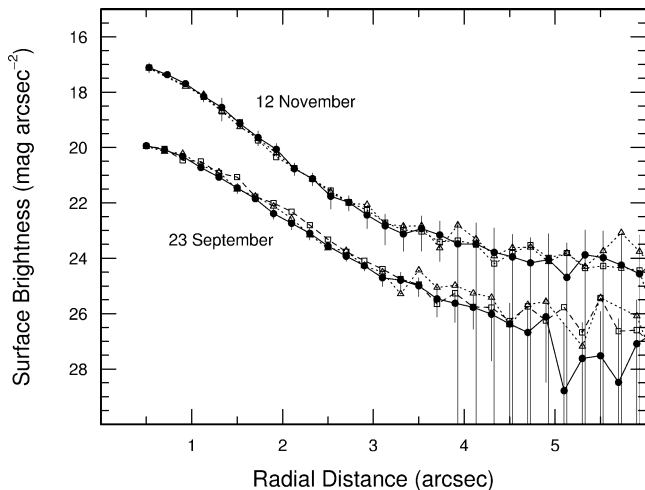


Fig. 3. Azimuthally averaged R-band radial profiles of 2001 PT₁₃ from 23 September and 12 November. 2001 PT₁₃ is represented by filled circles, and two comparison stars, scaled to the same peak brightness, are shown as open triangles and squares. Error bars on the comparison stars have been left off for clarity but are comparable to or slightly larger than those of 2001 PT₁₃. Also for clarity, the November data have been shifted up three units and 0.03 units to the right. The match between the Centaur and the two stars on both nights indicates that there is no detectable coma around 2001 PT₁₃.

stellar profiles could be measured. The total integration time of the composite images from September were 3300 s for the R-band image and 2700 s for the V-band image. For the November R and V composites, total times were 3600 s and 3300 s, respectively.

A visual inspection of these composite images indicated no obvious differences between 2001 PT₁₃ and the comparison stars. Likewise, contour plots of the Centaur were indistinguishable from those of comparison stars. A search for low surface brightness coma was done by extracting radial profiles of 2001 PT₁₃ and two nearby comparison stars of roughly the same magnitude. First, the sky background around each object was computed from an annulus between 50 and 100 pixels in radius. The background was flat to better than 0.1% across this dimension and pixels that varied by more than 2.5σ were rejected. The mode of the remaining pixels was adopted as the representative sky level and removed from the background behind the object. Next, azimuthally averaged radial profiles of 2001 PT₁₃ and the two stars were computed and are shown in Fig. 3, scaled to the same peak brightness. As can be seen, the radial profile of 2001 PT₁₃ is very close to those of the comparison stars, indicating that there is no detectable coma. In fact, the comparison stars have a slightly broader profile than 2001 PT₁₃, especially at distances beyond 3 arcsec, which is due to the slight amount of trailing that the stars experienced as we guided on the object.

As a final test, we looked for evidence of coma that might be concentrated in only one direction (e.g., a comet's tail), and is lost in the full azimuthal averages due to lack of contrast. For simplicity, we adopted four quadrants, defined by the four cardinal directions, and computed the additional ra-

dial profiles for both 2001 PT₁₃ and the comparison stars. (We did not focus on the anti-solar direction because with the large distances, slow velocities, and extreme projection effects involved in looking at objects at large heliocentric distance, there is only a small probability that tail material will be observed along the instantaneous projection of the anti-solar direction.) Again, there was no evidence for coma in any of the radial profiles.

Even though there is no evidence for coma, we can use the nondetection to set an upper limit on the dust production rate. We utilize the analysis presented in Davies et al. (1998b), which relates the dust production rate, \dot{M} (g s^{-1}), to the surface brightness of the coma, B ($\text{erg cm}^{-2} \text{s}^{-1} \text{\AA}^{-1}$)

$$\dot{M} = 3.750 \times 10^{23} \frac{\Delta^2 r^2}{p_0^2 S_0} \frac{B a \rho v_t R_0}{A},$$

where Δ and r are the geocentric and heliocentric distances to the object (AU), p_0 is the pixel size at the distance of the object (km), S_0 is the solar constant at 1 AU ($143 \text{ erg cm}^{-2} \text{s}^{-1} \text{\AA}^{-1}$), a is the dust grain radius (μm), ρ is the grain density (g cm^{-3}), v_t is the terminal velocity of the dust (km s^{-1}), R_0 is the distance from the Centaur projected onto the sky (km) and A is the dust albedo. Because we have no constraints on the dust parameters, we simply adopt reasonable values: $a = 0.5$, $\rho = 1.0$, $v_t = 0.1$, and $A = 0.05$, and recognize that each of these parameters has a linear effect on the production rate. Δ and r are listed in Table 1, and the pixel sizes, p_0 , are 3317 km and 3594 km for the September and November images, respectively (from which R_0 can be computed for a given pixel). Using the 1σ noise level for each annulus to give the surface brightness, we computed the dust production rates for both dates ($B = c \times 3.24 \times 10^{-22}$ on 23 September and $B = c \times 1.59 \times 10^{-22}$ on 12 November, where c is the count level). With these parameters, we compute an upper limit on the dust production of 15 g s^{-1} in September and 5 g s^{-1} in November (in both cases, this represents the maximum of all measurements within 6 arcsec). These levels will change if the adopted dust parameters do not represent the true coma, but it is clear that 2001 PT₁₃ is essentially an inactive body.

4. Discussion

The multi-wavelength lightcurve that we assembled was used to determine a number of the fundamental properties of 2001 PT₁₃. The average absolute magnitudes of the lightcurve are $H_R = 8.80$ and $H_V = 9.30$ (for an assumed $G = 0.15$). At present, there is no measurement of the albedo, but if we assume a value of 4%, then the effective diameter of 2001 PT₁₃ is about 90 km. (An albedo of 20% gives a diameter of only 40 km.)

Our PDM analysis of the lightcurve indicates that 2001 PT₁₃ has a rotation period of 0.34741 ± 0.00005 day and a double-peaked lightcurve with peaks of slightly different

amplitude. (Although a single-peaked lightcurve with a period of 0.1737 day is mathematically possible, the asymmetry of the two maxima is strong evidence for the double-peaked solution being the correct interpretation.) Our result is a more accurate determination than that presented by Ortiz et al. (2002) (0.346 ± 0.002 h), but the two results agree to within the uncertainties. Given the double-peaked lightcurve, 2001 PT₁₃ is an elongated body, with brightness variations produced by the changing apparent cross-section as it rotates. If we assume that the object can be represented by a prolate spheroid, then the 0.18 mag photometric range of the lightcurve indicates that the axial ratio a/b must be at least 1.18. (Due to foreshortening, a larger axial ratio would be necessary if the spin axis is not oriented in the plane of the sky.) The fact that the peaks are of slightly different amplitudes, however, suggests that the shape may deviate in some manner from a prolate spheroid.

Although, technically, our lightcurve analysis determined the synodic rotation period, the viewing geometry changed very little during our observations, which means that our result is a very close approximation to the sidereal rotation period. The fact that the lightcurve is essentially identical over a time span of three months indicates that 2001 PT₁₃ is in (or very near) a state of simple rotation about its short axis. Any complex rotation or precession acting on time scales of less than about a year would introduce shifts in the lightcurves from different observing runs, yet we see no evidence of this in our result.

Collisional models (e.g., Melosh and Ryan, 1997; Asphaug, 1998) show that it is much easier to disrupt a planetesimal larger than 250 m than to disperse the fragments. This suggests that many, if not most, large planetesimals are gravitationally bound rubble piles. Indirect observational evidence (e.g., Harris, 1996) supporting this theory includes the fact that asteroid rotation rates tend to be concentrated in the 8–10 hour range, with very few objects spinning faster than the critical rate for densities of 2.7 g cm^{-3} . Also, many large planetesimals are elongated, which might indicate that rotation is distorting their shapes. 2001 PT₁₃ fits both of these observational criteria, suggesting that it is also a candidate for a gravitationally bound rubble pile.

As described earlier, we computed VRJHK color indices for 2001 PT₁₃. In general our results are in good agreement with the data of Barucci et al. (2002), with our V–R, J–H and H–K colors consistent within the likely errors. There is a small but systematic difference in the absolute values of the near-IR magnitudes in the two data sets that cannot be accounted for by lightcurve variations. These may be attributable to subtle spectral variations across the surface or as yet unidentified differences in filters, reduction techniques or the values adopted for the standard stars.

The colors of 2001 PT₁₃ are consistent with typical values of the grey Centaur/KBO population, as well as with the colors of 1996 PW, 1998 WU₂₄ and 1999 LD₃₁ (Davies et al., 1998b, 2001; Harris et al., 2001). These latter three objects are in cometary-type orbits, but have, as yet, shown no

evidence of activity. It is possible that they represent a different stage in the evolution of the Centaurs. A plot of V–R as a function of rotational phase shows no evidence for color variations at optical wavelengths across the surface of 2001 PT₁₃. A similar plot of R–J colors hints that there may be some variations at longer wavelengths, but further investigation is needed to confirm this.

Our search for coma around 2001 PT₁₃ revealed no significant evidence for activity, even though the Centaur was close to perihelion during our observations. On the other hand, Chiron's activity was not observed until two years after perihelion and has persisted for over a decade. This suggests that the activity is driven by thermal energy propagating into the interior where phase changes in amorphous water ice may result in the release of occluded CO molecules (Prialnik et al., 1995). Given this delay in Chiron's activity, it may be worth following up on observations of 2001 PT₁₃ and other Centaurs to determine if they exhibit activity in the years after perihelion.

Finally, we note that two near-IR spectra of 2001 PT₁₃, obtained on two different dates (September and October 2001) by Barucci et al. (2002), seem to exhibit dramatic differences. With our period determination, we find that the first of these spectra was obtained when 2001 PT₁₃ was at a rotational phase of 0.06 and the second when it was at a phase of 0.48. Thus, the two spectra were obtained nearly half a rotation apart, and represent opposite ends of 2001 PT₁₃. The difference in the spectra, combined with the possible color variations in our R–J colors as a function of the rotation (Fig. 2) may indicate that there are inhomogeneities across the object's surface at near-IR wavelengths. Barucci et al. (2002) also observed a possible signature for water ice in one of their spectra. This is intriguing, though 2001 PT₁₃ is at a heliocentric distance well beyond the distance at which water begins to sublimate at any significant rate (e.g., Delsemme, 1982, and references therein), so sublimation of this surface ice should not be expected to generate much cometary activity. In any case, this makes the Centaur a very interesting object, for which follow-up observations should be obtained.

If the dramatic differences seen in spectra are indeed real, then we can invert the above argument and use the differing spectra to set a constraint on the pole orientation of 2001 PT₁₃. First, we note that each spectrum represents the disk-integrated light for the phase at which it was obtained. Because they show dramatic differences, the two spectra must, therefore, represent very different faces of the Centaur, suggesting that we are seeing 2001 PT₁₃ from a sub-Earth latitude near its equator. With this configuration, the phase shift between the two spectra would have presented nearly opposing hemispheres, as assumed above, and one face would be hidden while the other is in view. In the alternate case, if the sub-Earth latitude were near the pole, then most of the visible face of the object would remain the same throughout a rotation. With this configuration, dramatic spectral differences would not be likely, because most

of the disk-integrated light would be the same from one phase to another. Therefore, we conclude that the spin axis of 2001 PT₁₃ is probably near the plane of the sky. Additional constraints should be possible in the next few years as the viewing geometry changes (e.g., Farnham, 2001b). If the pole is near the plane of the sky, then we can also conclude that the changing apparent cross-section as a function of rotation is not affected very much by foreshortening effects. Thus, 2001 PT₁₃ is not highly elongated and is likely to have an axial ratio, a/b , near the 1.18 limit computed from the lightcurve amplitude.

Acknowledgments

We would like to thank A. Barucci and co-authors for making available their results prior to publication. JKD thanks the staff of the Joint Astronomy Centre in Hilo for their typically thorough and professional assistance during the UKIRT observing run. Lisa Ferris (Institute for Astronomy, Edinburgh) made a useful contribution to the UKIRT data reduction as part of her undergraduate project work. We also appreciate the helpful comments from Dr. Karen Meech and Dr. Simon Green, who refereed the manuscript.

The United Kingdom Infrared Telescope is operated by the Joint Astronomy Centre on behalf of the UK Particle Physics and Astronomy Research Council.

Image processing in this paper has been performed using the IRAF program. IRAF is distributed by the National Optical Astronomy Observatories, which is operated by the Association of Universities for Research in Astronomy, Inc. (AURA) under cooperative agreement with the National Science Foundation.

This research was funded, in part, by NASA Grant NAG5-4384.

References

- Asphaug, E., 1998. Disruption of planetesimals by tides and collisions. *Bull. Am. Ast. Soc.* 30, 1027.
- Barucci, M., Boehnhardt, H., Dotto, E., Doressoundiram, A., Romon, J., Lazzarin, M., Fornasier, S., de Bergh, C., Tozzi, G., Delsanti, A., Hainaut, O., Barrera, L., Birkle, K., Meech, K., Ortiz, J., Sekiguchi, T., Thomas, N., Watanabe, J., West, R., Davies, J., 2002. Visible and near infrared spectroscopy of the Centaur 32532 (2001 PT₁₃) I. ESO TNO large Program, first spectroscopy results. *Astron. Astrophys.* 392, 335–339.
- Bauer, J.M., Meech, K.J., Fernández, Y.R., Farnham, T.L., Roush, T.L., 2002. Observations of the Centaur 1999 UG₅: evidence of a unique outer Solar System surface. *Publ. Astron. Soc. Pacific* 114, 1309–1321.
- Bowell, E., Hapke, B., Domingue, D., Lumme, K., Peltoniemi, K., Harris, A., 1989. Application of photometric models to asteroids. I. In: Binzel, R., Gehrels, T., Matthews, M. (Eds.), *Asteroids II*. Univ. of Arizona Press, Tucson, pp. 549–554.
- Bridger, A., Wright, G.S., Economou, F., Tan, M., Currie, M.J., Pickup, D.A., Adamson, A.J., Rees, N.P., Purves, M., Kackley, R., 2000. ORAC: a modern observing system for UKIRT. In: Lewis, H. (Ed.), *Proc. SPIE: Advanced Telescope and Instrumentation Control Software*, Vol. 4009, pp. 227–238.
- Brown, M.E., Koresko, C.C., 1998. Detection of water ice on the Centaur 1997 CU 26. *Astrophys. J.* 505, L65–L67.
- Cruikshank, D., Roush, T., Bartholomew, M., Geballe, T., Pendleton, Y., White, S., Bell, J., Davies, J., Owen, T., de Bergh, C., Tholen, D., Bernstein, M., Brown, R., Tryka, K., Dalle Ore, C., 1998. The composition of 5145 Pholus. *Icarus* 135, 389–407.
- Currie, M.J., 2001. ORAC-DR Imaging Data Reduction. CCLRC/Rutherford Appleton Laboratory, Hilo, HI.
- Davies, J., McBride, N., Ellison, S., Green, S., Ballantyne, D., 1998a. Visible and infrared photometry of six Centaurs. *Icarus* 134, 213–227.
- Davies, J., McBride, N., Green, S., Mottola, S., Carsent, U., Basran, D., Hudson, K., Foster, M., 1998b. The lightcurve and colors of unusual minor planet 1996 PW. *Icarus* 132, 418–430.
- Davies, J., Tholen, D., Whiteley, R., Green, S., Hillier, J., Foster, M., McBride, N., Kerr, T., Muzzerall, E., 2001. The lightcurve and colors of unusual minor planet 1998 WU₂₄. *Icarus* 150, 69–77.
- Delsemme, A.H., 1982. Chemical composition of cometary nuclei. In: Wilkening, L.L. (Ed.), *Comets*. Univ. of Arizona Press, Tucson, pp. 85–130.
- Farnham, T.L., 2001a. Rotation and color studies of Centaurs, KBOs and comets. *Bull. Am. Ast. Soc.* 33, 1047.
- Farnham, T.L., 2001b. The rotation axis of the Centaur 5145 Pholus. *Icarus* 152, 238–245.
- Foster, M.J., Green, S.F., McBride, N., Davies, J.K., 1999. Detection of water ice on 2060 Chiron. *Icarus* 141, 408–410.
- Harris, A.W., 1996. The rotation rates of very small asteroids: evidence for ‘rubble pile’ structure. In: *Lunar and Planetary Institute Conference Abstracts*, Vol. 27, pp. 493–494.
- Harris, A.W., Delbó, M., Binzel, R.P., Davies, J.K., Roberts, J., Tholen, D.J., Whitely, R.J., 2001. Visible to thermal infrared spectrophotometry of a possible inactive comet nucleus. *Icarus* 153, 332–337.
- Hawarden, T.G., Leggett, S.K., Letawsky, M.B., Ballantyne, D.R., Casali, M.M., 2001. JHK standard stars for large telescopes: the UKIRT fundamental and extended lists. *Mon. Not. R. Astron. Soc.* 325, 563–574.
- Kern, S.D., McCarthy, D.W., Buie, M.W., Brown, R.H., Campins, H., Rieke, M., 2000. Compositional variation on the surface of Centaur 8405 Asbolus. *Astrophys. J.* 542, L155–L159.
- Landolt, A., 1992. UBVRI photometric standard stars in the magnitude range 11.5–16.0 around the celestial equator. *Astron. J.* 104, 340–371.
- Luu, J.X., Jewitt, D.C., 1990. Cometary activity in 2060 Chiron. *Astron. J.* 100, 913–932.
- Luu, J.X., Jewitt, D.C., Trujillo, C., 2000. Water ice in 2060 Chiron and its implications for Centaurs and Kuiper Belt objects. *Astrophys. J.* 531, L151–L154.
- Meech, K.J., Belton, M.J.S., 1989. (2060) Chiron. *IAU Circ.* 4770.
- Meech, K.J., Buie, M.W., Samarasinha, N.H., Mueller, B.E.A., Belton, M.J.S., 1997. Observations of structures in the inner coma of Chiron with the HST planetary camera. *Astron. J.* 113, 844–862.
- Melosh, H.J., Ryan, E.V., 1997. Asteroids: shattered but not dispersed. *Icarus* 129, 562–564.
- Ortiz, J.L., Baumont, S., Gutiérrez, P.J., Roos-Serote, M., 2002. Lightcurves of Centaurs 2000 QC₂₄₃ and 2001 PT₁₃. *Astron. Astrophys.* 388, 661–666.
- Pravdo, S., Heline, E., Hicks, M., Lawrence, K., 2001. Comet C/2001 T4 (NEAT). *IAU Circ.* 7738.
- Prialnik, D., Brosch, N., Ianovici, D., 1995. Modelling the activity of 2060 Chiron. *Mon. Not. R. Astron. Soc.* 276, 1148–1154.
- Schulz, R., 2002. Trans-neptunian objects. *Astron. Astrophys. Rev.* 11, 1–31.
- Stellingwerf, R., 1978. Period determination using phase dispersion minimization. *Astrophys. J.* 224, 953–960.